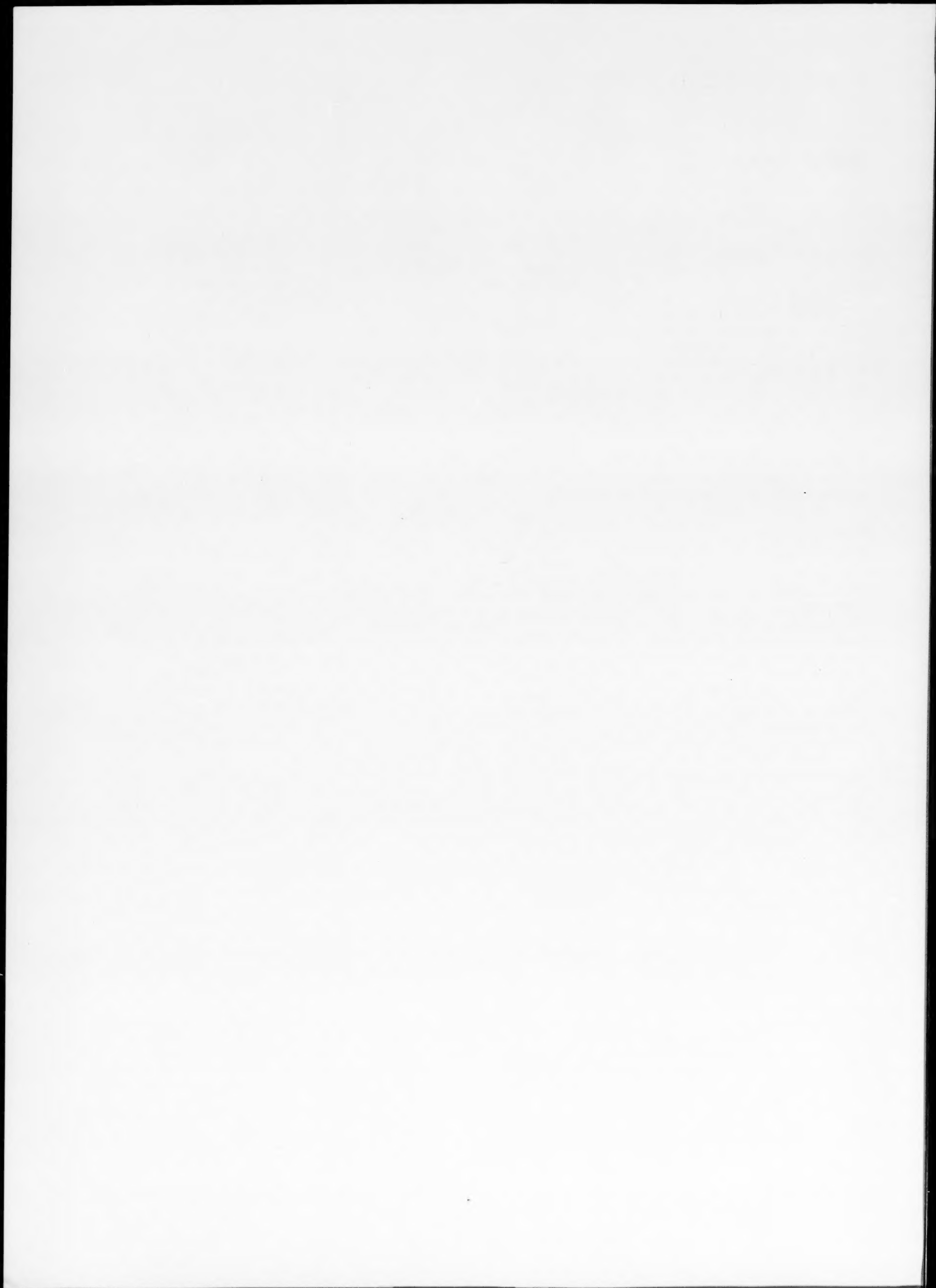


Author Index

- Ai, S. H., 141
Arsenault, R. J., 285, 291
- Baskes, M. I., 289
Bassim, M. N., 81, 241
Beniska, J., 63
Berglin, L., 87
Bowen, H. K., 213
Brown, L. M., 281
Buck, O., 117
- Chang, Y. J., 81, 241
Chen, D. L., 141
Chrysochoos, A., 25
- Dybiec, H., 97
- Esterling, D. M., 291
Exner, H. E., 121
- Fortes, M. A., 1
Fujimura, N., 153
- Gabb, T. P., 189
Gao, Y.-Q., 19
Gayda, J., 189
Gottstein, G., 165
Gruner, H., 87, 105
Gudmundsson, B., 73, 87, 105, 181
- Hay, R. A., 213
Hudec, I., 63
Hunderi, O., 33
- Ito, T., 153
- Jacobson, B. E., 73, 87, 105, 181
Jiang, X. X., 141
- Karunanithy, S., 221
Kassner, M. E., 45
Kim, W., 165
- Laird II, G., L1
L'Estrade, L., 87
Langer, E. W., 247
Liu, C. Y., 265
Liu, X., 19
Lo, Y.-B., 19
Lynch, S. P., 203
- Macmillan, N. H., L1
Martin, G., 25
McQueen, H. J., 45
Miner, R. V., 189
Miranda, R. M., 1
Moffat, W. C., 213
Murakami, K., 265, 271
Myshlyaev, M. M., 45
- Nagpal, P., 165
Nakayama, Y., 153
Nakazono, S., 271
Nishida, N., 153
- Okamoto, T., 265, 271
Owen, C. V., 117
- Pawłowski, A., 9
Pedersen, O. B., 281
- Raphanel, J. L., 227
Rdzawski, Z., 97
Richert, M., 97
Roliński, E., 37
Rosner, P., 63
Ryum, N., 33
- Sadananda, K., 131
Saetre, T. O., 33
Sain, M. M., 63
Sanchez, J. M., 159
Schmitt, J.-H., 227
Seigle, L. L., 253
Shahinian, P., 131
Shih, C. H., 141
Shume, A. J., 81, 241
Sigl, L. S., 121
Stobbs, W. M., 281
- Taya, M., 285
Tso, N. C., 159
- Van Houtte, P., 227
- Wang, T. H., 253
Wang, W., 19
Wang, Z. G., 141
Welsch, G., 189
Withers, P. J., 281
- Yang, X.-Q., 19
- Zenkert, D., 233
Zhuang, L. Z., 247
Zięba, P., 9



Subject Index

Age-hardening

- flow stress and structure of age-hardened Cu-0.4wt.%Cr alloy after large deformation, 97

Alloys

- creep and fatigue crack growth behavior of some cast nickel-base alloys, 131
- flow stress and structure of age-hardened Cu-0.4wt.%Cr alloy after large deformation, 97
- internal and external shrinkages in unidirectionally solidified Al-4.5wt.%Cu alloy, 265
- low temperature hydrogen effects on the strength and ductility of Nb-Ta alloys, 117
- mechanism of early stages of discontinuous dissolution in AlZn alloys, 9
- self-annealing of rapidly solidified deposit layers of Fe-C-Si alloys by flame spraying, 271
- solid-metal-induced embrittlement of aluminium alloys and other materials, 203
- surface properties of plasma-nitrided titanium alloys, 37
- the influence of substrate temperature on the microstructure and hardness of vacuum-plasma-sprayed Co-Ni-Cr-Al-Si-Zn-Y and Co-Ni-Cr-Al-Y alloys, 105
- the kinetics of pack aluminization of iron from Al-Fe alloy packs, 253

Aluminium

- comments on "The Strength Differential and Bauschinger Effects in SiC-Al Composites", 281
- effects of texture in the titanium layer on solid state reactions for Al/Ti/Si and Al/TiN/Ti/Si systems, 153
- further comments on "The Strength Differential and Bauschinger Effects in SiC-Al Composites", 285
- internal and external shrinkages in unidirectionally solidified Al-4.5wt.%Cu alloy, 265
- large-strain torsional deformation in aluminum at elevated temperatures, 45
- mechanism of early stages of discontinuous dissolution in AlZn alloys, 9
- microstructure and erosion resistance of vacuum-plasma-sprayed Co-Ni-Cr-Al-Y/Al₂O₃ composite coatings, 87
- recrystallization and texture in boron-doped Ni₃Al, 165
- reinforcement of carbon fibre-alumina composite interfaces, 221
- sintering behavior of uniform-sized α -Al₂O₃ powder, 213
- solid-metal-induced embrittlement of aluminium alloys and other materials, 203
- the effect of silicon and zirconium additions on the microstructure of vacuum-plasma-sprayed Co-Ni-Cr-Al-Y coatings, 73
- the influence of substrate temperature on the microstructure and hardness of vacuum-plasma-sprayed Co-Ni-Cr-Al-Si-Zn-Y and Co-Ni-Cr-Al-Y alloys, 105
- the kinetics of pack aluminization of iron from Al-Fe alloy packs, 253
- the orientation relationship between γ (f.c.c.) and β -NiAl in vacuum-plasma-sprayed Co-Ni-Cr-Al-Y coatings, 181

- thermodynamic modeling of site occupation in the γ' phase of the Ni-Al-Hf system, 159

Annealing

- self-annealing of rapidly solidified deposit layers of Fe-C-Si alloys by flame spraying, 271

Austenite

- austenite grain growth, microstructure and hardness in the heat-affected zone of a 2.25Cr-1Mo steel, 1

Bauschinger effect

- comments on "The Strength Differential and Bauschinger Effects in SiC-Al Composites", 281
- further comments on "The Strength Differential and Bauschinger Effects in SiC-Al Composites", 285

Boron

- recrystallization and texture in boron-doped Ni₃Al, 165

Carbon

- comments on "The Strength Differential and Bauschinger Effects in SiC-Al Composites", 281
- further comments on "The Strength Differential and Bauschinger Effects in SiC-Al Composites", 285
- reinforcement of carbon fibre-alumina composite interfaces, 221
- self-annealing of rapidly solidified deposit layers of Fe-C-Si alloys by flame spraying, 271

Chromium

- austenite grain growth, microstructure and hardness in the heat-affected zone of a 2.25Cr-1Mo steel, 1
- determination of cyclic strain-hardening behaviour produced during fatigue crack growth in cast Co-Cr-Mo alloy used for surgical implants, 247
- flow stress and structure of age-hardened Cu-0.4wt.%Cr alloy after large deformation, 97
- microstructure and erosion resistance of vacuum-plasma-sprayed Co-Ni-Cr-Al-Y/Al₂O₃ composite coatings, 87
- the effect of silicon and zirconium additions on the microstructure of vacuum-plasma-sprayed Co-Ni-Cr-Al-Y coatings, 73
- the influence of substrate temperature on the microstructure and hardness of vacuum-plasma-sprayed Co-Ni-Cr-Al-Si-Zn-Y and Co-Ni-Cr-Al-Y alloys, 105
- the orientation relationship between γ (f.c.c.) and β -NiAl in vacuum-plasma-sprayed Co-Ni-Cr-Al-Y coatings, 181

Cobalt

- determination of cyclic strain-hardening behaviour produced during fatigue crack growth in cast Co-Cr-Mo alloy used for surgical implants, 247
- microstructure and erosion resistance of vacuum-plasma-sprayed Co-Ni-Cr-Al-Y/Al₂O₃ composite coatings, 87
- the effect of silicon and zirconium additions on the microstructure of vacuum-plasma-sprayed Co-Ni-Cr-Al-Y coatings, 73

- the influence of substrate temperature on the microstructure and hardness of vacuum-plasma-sprayed Co-Ni-Cr-Al-Si-Zn-Y and Co-Ni-Cr-Al-Y alloys, 105
- the orientation relationship between γ (f.c.c.) and β -NiAl in vacuum-plasma-sprayed Co-Ni-Cr-Al-Y coatings, 181
- Composites**
- comments on "The Strength Differential and Bauschinger Effects in SiC-Al Composites", 281
- further comments on "The Strength Differential and Bauschinger Effects in SiC-Al Composites", 285
- microstructure and erosion resistance of vacuum-plasma-sprayed Co-Ni-Cr-Al-Y/ Al_2O_3 composite coatings, 87
- reinforcement of carbon fibre-alumina composite interfaces, 221
- the flow stress and hardness of metal-reinforced brittle composites, 121
- Copper**
- a study of the effect of initial grain size and strain rate on dislocation structures in copper, 241
- crystallization behavior of $\text{Ti}_{66.6}\text{Ni}_{13.6}\text{Cu}_{12.5}\text{Ge}_{7.3}$ glass, 19
- flow stress and structure of age-hardened Cu-0.4wt.%Cr alloy after large deformation, 97
- fracture topography of commercial copper, 81
- internal and external shrinkages in unidirectionally solidified Al-4.5wt.%Cu alloy, 265
- Crack growth**
- creep and fatigue crack growth behavior of some cast nickel-base alloys, 131
- determination of cyclic strain-hardening behaviour produced during fatigue crack growth in cast Co-Cr-Mo alloy used for surgical implants, 247
- the dependence of near-threshold fatigue crack growth on microstructure and environment in dual-phase steels, 141
- Creep**
- creep and fatigue crack growth behavior of some cast nickel-base alloys, 131
- Crystallization**
- crystallization behavior of $\text{Ti}_{66.6}\text{Ni}_{13.6}\text{Cu}_{12.5}\text{Ge}_{7.3}$ glass, 19
- Deformation**
- flow stress and structure of age-hardened Cu-0.4wt.%Cr alloy after large deformation, 97
- large-strain torsional deformation in aluminum at elevated temperatures, 45
- the low cycle fatigue deformation response of a single-crystal superalloy at 650 °C, 189
- Dislocation**
- a study of the effect of initial grain size and strain rate on dislocation structures in copper, 241
- an atomistic study of the relationship between stacking fault energy and partial dislocation splitting, 289
- comments on "An atomistic study of the relationship between stacking fault energy and partial dislocation splitting", 291
- Dissolution**
- mechanism of early stages of discontinuous dissolution in AlZn alloys, 9
- Ductility**
- low temperature hydrogen effects on the strength and ductility of Nb-Ta alloys, 117
- Embrittlement**
- solid-metal-induced embrittlement of aluminium alloys and other materials, 203
- Erosion**
- microstructure and erosion resistance of vacuum-plasma-sprayed Co-Ni-Cr-Al-Y/ Al_2O_3 composite coatings, 87
- Fatigue**
- creep and fatigue crack growth behavior of some cast nickel-base alloys, 131
- determination of cyclic strain-hardening behaviour produced during fatigue crack growth in cast Co-Cr-Mo alloy used for surgical implants, 247
- the dependence of near-threshold fatigue crack growth on microstructure and environment in dual-phase steels, 141
- the low cycle fatigue deformation response of a single-crystal superalloy at 650 °C, 189
- Fracture**
- fracture topography of commercial copper, 81
- poly(vinyl chloride) sandwich core materials: fracture behaviour under mode II loading and mixed-mode conditions, 233
- Germanium**
- crystallization behavior of $\text{Ti}_{66.6}\text{Ni}_{13.6}\text{Cu}_{12.5}\text{Ge}_{7.3}$ glass, 19
- Grain growth**
- austenite grain growth, microstructure and hardness in the heat-affected zone of a 2.25Cr-1Mo steel, 1
- the effect of grain boundary edges on grain growth and grain growth stagnation, 33
- Hafnium**
- thermodynamic modeling of site occupation in the γ' phase of the Ni-Al-Hf system, 159
- Hardness**
- austenite grain growth, microstructure and hardness in the heat-affected zone of a 2.25Cr-1Mo steel, 1
- the flow stress and hardness of metal-reinforced brittle composites, 121
- Heterogeneity**
- contribution to heterogeneity in elasto-plastic blends, 63
- Hydrogen**
- low temperature hydrogen effects on the strength and ductility of Nb-Ta alloys, 117
- Iron**
- self-annealing of rapidly solidified deposit layers of Fe-C-Si alloys by flame spraying, 271
- the kinetics of pack aluminization of iron from Al-Fe alloy packs, 253
- Microstructure**
- austenite grain growth, microstructure and hardness in the heat-affected zone of a 2.25Cr-1Mo steel, 1
- microstructure and erosion resistance of vacuum-plasma-sprayed Co-Ni-Cr-Al-Y/ Al_2O_3 composite coatings, 87
- the dependence of near-threshold fatigue crack growth on microstructure and environment in dual-phase steels, 141

- the influence of substrate temperature on the microstructure and hardness of vacuum-plasma-sprayed Co-Ni-Cr-Al-Si-Zn-Y and Co-Ni-Cr-Al-Y alloys, 105
- Molybdenum**
- austenite grain growth, microstructure and hardness in the heat-affected zone of a 2.25Cr-1Mo steel, 1
 - determination of cyclic strain-hardening behaviour produced during fatigue crack growth in cast Co-Cr-Mo alloy used for surgical implants, 247
- Nickel**
- creep and fatigue crack growth behavior of some cast nickel-base alloys, 131
 - crystallization behavior of $\text{Ti}_{66.6}\text{Ni}_{13.6}\text{Cu}_{12.5}\text{Ge}_{7.3}$ glass, 19
 - microstructure and erosion resistance of vacuum-plasma-sprayed Co-Ni-Cr-Al-Y/ Al_2O_3 composite coatings, 87
 - recrystallization and texture in boron-doped Ni_3Al , 165
 - the effect of silicon and zirconium additions on the microstructure of vacuum-plasma-sprayed Co-Ni-Cr-Al-Y coatings, 73
 - the influence of substrate temperature on the microstructure and hardness of vacuum-plasma-sprayed Co-Ni-Cr-Al-Si-Zn-Y and Co-Ni-Cr-Al-Y alloys, 105
 - the orientation relationship between γ (f.c.c.) and β -NiAl in vacuum-plasma-sprayed Co-Ni-Cr-Al-Y coatings, 181
 - thermodynamic modeling of site occupation in the γ' phase of the Ni-Al-Hf system, 159
- Niobium**
- low temperature hydrogen effects on the strength and ductility of Nb-Ta alloys, 117
- Nitrogen**
- effects of texture in the titanium layer on solid state reactions for Al/Ti/Si and Al/TiN/Ti/Si systems, 153
 - surface properties of plasma-nitrided titanium alloys, 37
- Oxygen**
- flow stress and structure of age-hardened Cu-0.4wt.%Cr alloy after large deformation, 97
 - reinforcement of carbon fibre-alumina composite interfaces, 221
- Poly(vinyl chloride)**
- poly(vinyl chloride) sandwich core materials: fracture behaviour under mode II loading and mixed-mode conditions, 233
- Recrystallization**
- recrystallization and texture in boron-doped Ni_3Al , 165
- Reinforcement**
- reinforcement of carbon fibre-alumina composite interfaces, 221
 - the flow stress and hardness of metal-reinforced brittle composites, 121
- Shrinkages**
- internal and external shrinkages in unidirectionally solidified Al-4.5wt.%Cu alloy, 265
- Silicon**
- comments on "The Strength Differential and Bauschinger Effects in SiC-Al Composites", 285
 - effects of texture in the titanium layer on solid state reactions for Al/Ti/Si and Al/TiN/Ti/Si systems, 153
 - further comments on "The Strength Differential and Bauschinger Effects in SiC-Al Composites", 285
 - self-annealing of rapidly solidified deposit layers of Fe-C-Si alloys by flame spraying, 271
 - the effect of silicon and zirconium additions on the microstructure of vacuum-plasma-sprayed Co-Ni-Cr-Al-Y coatings, 73
 - the influence of substrate temperature on the microstructure and hardness of vacuum-plasma-sprayed Co-Ni-Cr-Al-Si-Zn-Y and Co-Ni-Cr-Al-Y alloys, 105
- Single crystals**
- the low cycle fatigue deformation response of a single-crystal superalloy at 650 °C, 189
- Sintering**
- sintering behavior of uniform-sized α - Al_2O_3 powder, 213
- Stacking faults**
- an atomistic study of the relationship between stacking fault energy and partial dislocation splitting, 289
 - comments on "An atomistic study of the relationship between stacking fault energy and partial dislocation splitting", 291
- Strain**
- a study of the effect of initial grain size and strain rate on dislocation structures in copper, 241
 - large-strain torsional deformation in aluminum at elevated temperatures, 45
- Strain-hardening**
- determination of cyclic strain-hardening behaviour produced during fatigue crack growth in cast Co-Cr-Mo alloy used for surgical implants, 247
- Strength differential**
- texture development and strength differential effect in textured b.c.c. metals with glide asymmetry, 227
 - comments on "The Strength Differential and Bauschinger Effects in SiC-al Composites", 281
 - further comments on "The Strength Differential and Bauschinger Effects in SiC-Al Composites", 285
- Stress**
- flow stress and structure of age-hardened Cu-0.4wt.%Cr alloy after large deformation, 97
 - the flow stress and hardness of metal-reinforced brittle composites, 121
- Tantalum**
- low temperature hydrogen effects on the strength and ductility of Nb-Ta alloys, 117
- Tensile testing**
- tensile test microcalorimetry for thermomechanical behaviour law analysis, 25
- Texture**
- effects of texture in the titanium layer on solid state reactions for Al/Ti/Si and Al/TiN/Ti/Si systems, 153
 - recrystallization and texture in boron-doped Ni_3Al , 165
 - texture development and strength differential effect in textured b.c.c. metals with glide asymmetry, 227
- Thermodynamic modeling**
- thermodynamic modeling of site occupation in the γ' phase of the Ni-Al-Hf system, 159
- Titanium**
- crystallization behavior of $\text{Ti}_{66.6}\text{Ni}_{13.6}\text{Cu}_{12.5}\text{Ge}_{7.3}$ glass, 19
 - effects of texture in the titanium layer on solid state reactions for Al/Ti/Si and Al/TiN/Ti/Si systems, 153
 - surface properties of plasma-nitrided titanium alloys, 37

Yttrium

- microstructure and erosion resistance of vacuum-plasma-sprayed Co-Ni-Cr-Al-Y/ Al_2O_3 composite coatings, 87
- the effect of silicon and zirconium additions on the microstructure of vacuum-plasma-sprayed Co-Ni-Cr-Al-Y coatings, 73
- the influence of substrate temperature on the microstructure and hardness of vacuum-plasma-sprayed Co-Ni-Cr-Al-Si-Zn-Y and Co-Ni-Cr-Al-Y alloys, 105
- the orientation relationship between γ (f.c.c.) and β -NiAl in vacuum-plasma-sprayed Co-Ni-Cr-Al-Y coatings, 181

Zinc

- mechanism of early stages of discontinuous dissolution in AlZn alloys, 9
- the influence of substrate temperature on the microstructure and hardness of vacuum-plasma-sprayed Co-Ni-Cr-Al-Si-Zn-Y and Co-Ni-Cr-Al-Y alloys, 105

Zirconium

- the effect of silicon and zirconium additions on the microstructure of vacuum-plasma-sprayed Co-Ni-Cr-Al-Y coatings, 73

CONTENTS (continued)

BOOK REVIEWS	293
CONFERENCE CALENDAR	301
LETTER	
An approximate description of the temporal evolution of a Hertzian impact	L1
N. H. Macmillan and G. Laird II (Albany, OR, U.S.A.)	
AUTHOR INDEX	307
SUBJECT INDEX	309

